



## Effects of Experimental Nano-Hydroxyapatite Pastes on Remineralization of Early Demineralized Enamel

Amornthep Vacharangkura<sup>1</sup> and Sitthikorn Kunawarote<sup>\*2</sup>

<sup>1</sup>Restorative Dentistry Section Faculty of Dentistry, Chiang Mai University, Chiang Mai, Thailand

<sup>2</sup>Department of Restorative Dentistry and Periodontal Dentistry, Faculty of Dentistry, Chiang Mai University, Chiang Mai, Thailand

\*Corresponding author, E-mail: [sitthikorn.k@cmu.ac.th](mailto:sitthikorn.k@cmu.ac.th)

### Abstract

This study aims to evaluate the remineralization effects of nano-hydroxyapatite paste on the early demineralized enamel under a simulated pH cycling model compared with fluoride paste. Enamel specimens were obtained from human premolars and embedded in acrylic resin blocks. All specimens were ground flat and subjected to demineralized for 7 days to create the early demineralized lesion prior to the perpendicular sectioned through the surface for measuring mineral loss. Forty-eight specimens with an average of mineral loss were selected and randomly allocated to three groups (n=16): control (without treatment), nano-hydroxyapatite paste (10% HAP), and fluoride paste (1000 ppm NaF). Mineral loss ( $\Delta Z$ ) and lesion depth (LD) were analyzed using micro-computed tomography. All specimens were evaluated after assigned treatment and simulated pH cycling model for 7 and 14 days. Within the experimental group, mineral loss and lesion depth were examined at the period of 7 and 14 days with one-way ANOVA. All collected data were calculated for the resulting changes in mineral loss ( $\Delta\Delta Z$ ) and lesion depth ( $\Delta LD$ ) and analyzed between the experimental groups and times with two ways ANOVA. All statistical analyses were performed at a 5% level of significance. The results showed that the nano-hydroxyapatite paste and fluoride paste exhibited the ability to diminish mineral loss and lesion depth significantly after treated for 14 days. On the other hand, the control group showed progress in mineral loss and lesion depth after a period of 7 and 14 days. In conclusion, the use of nano-hydroxyapatite paste under the condition of pH-cycling for 14 days promotes remineralization on early demineralized enamel in the same way as using fluoride paste. However, the different characteristics of remineralization should be observed.

**Keywords:** *Early demineralized enamel, Fluoride, micro-CT scan, Nano-hydroxyapatite, pH cycling model, Remineralization*

### 1. Introduction

Dental caries are the overall outcome of the cyclical demineralization and remineralization process, which continuously occurs between the biofilm and the tooth surface. The process of demineralization starts from acids obtained from bacterial carbohydrate metabolism, causing the dissolution of minerals at the tooth surface. Enamel is often the starting area of dental caries due to its being the outermost layer of the tooth. It is also a non-cellular tissue with the main component of 96% inorganics by weight. The rest is composed of organics and water. Hydroxyapatite is the main inorganic and the smallest subunit of enamel with prism formation (ten Cate & Featherstone, 1991). The space between prisms and crystals is home to water and organics of proteins and lipids (Oduyaga & Prout, 1974). Additionally, it is a channel for the diffusion of organic acids and free ions from the outer part of the teeth in the demineralization and remineralization process (Moreno & Zahradnik, 1973). Bacterial acids, therefore, utilize that channel to penetrate the subsurface and dissolve the minerals beneath the tooth surface, resulting in the enamel caries that start from non-cavitated lesions or white spot lesions and indicating the overall primary demineralization beneath the enamel subsurface. If not managed properly, the demineralization process continues over a long period of time until the adequate dissolution of minerals in the tooth surface is reached, which then develops into the cavitated lesion (Pitts, 2004).

White spot lesions are the first signs of dental caries lesions which can be clinically detected with the naked eye. The clinical characteristics include intact surface and non-cavitated, but softened surface hardness. The softened surface hardness of these lesions results from the remineralization of subsurface



lesions accumulating on the area of the outer surface (Kidd & Fejerskov, 2004). Thus, the examination of white spots is commonly observed by the changing color of lesions on humidity conditions. When the surface is wet, the lesions appear transparent due to the penetration of external water into the pores following the demineralization, with a refractive index close to the normal enamel. On the other hand, if the tooth surface is dry, the lesions become chalky white because of the remaining air-infiltrated pores with a very different refractive index from the enamel.

The current approach of conservative treatment focuses on a reinforcement of non-cavitated lesions for the longest functional ability. It is a minimally invasive treatment, instead of an extension for prevention, by promoting remineralization and inhibiting demineralization prior to the development of lesions to the cavitated enamel, which has to lose the tooth structure from the removal of tooth decay and filling (Murdoch-Kinch & McLean, 2003). In normal conditions, teeth can be remineralized by calcium and phosphate from saliva or biofilm with sufficient concentration to cause a supersaturate with respect to calcium and phosphate of hydroxyapatite crystals in the teeth, progressing to crystal formation on the old rather than new ones (Featherstone, 2000). However, it may not sufficiently lead to the overall remineralization in some cases because of a greater demineralization process. The use of agents to enhance remineralization or remineralizing agents is thus one of the methods to manage non-cavitated lesions or white spot lesions, focusing on the remineralization to the demineralized parts in the subsurface while maintaining their intact conditions (Featherstone, 2008). The examples of remineralizing agents include fluoride (Buzalaf, Pessan, Honorio, & ten Cate, 2011), casein phosphopeptides-amorphous calcium phosphate: CPP-ACP (Cochrane, Cai, Huq, Burrow, & Reynolds, 2010), and nano-hydroxyapatite (Tschoppe, Zandim, Martus, & Kielbassa, 2011; Yamagishi et al., 2005).

Using fluoride in caries prevention is very common nowadays, regarding its control and preventive efficiency (Adair, 2006; Bruun et al., 1985; Bruun, Lambrou, Larsen, Fejerskov, & Thylstrup, 1982). Fluoride plays a role in protecting against dental caries through three actions of mechanism. First, it inhibits demineralization from the ion exchange between fluoride ions and hydroxyapatite crystal surface (Featherstone, 1999), forming fluorapatite crystals that possess higher resistance to dissolution than hydroxyapatite (Arends & Christoffersen, 1990). This crystallization process can occur even in the solutions with a small amount of fluoride (Featherstone, Glena, Shariati, & Shields, 1990). Second, the enhancement of remineralization with the oral pH value higher than 5.5 in combination with even a small number of fluoride ions can penetrate the precipitation of damaged crystals for fluorohydroxyapatite crystals formation (Featherstone, 1999), thus accelerating the remineralization process. Besides, fluoride also binds to the surface of partially dissolved crystals and attracts calcium ions to repair the crystal surface, making these new crystals more resistant to acids than the old ones (Featherstone, 1999). Lastly, the inhibition of the metabolic process of caries-causing bacteria is done through the intra-cellular enzyme inhibition with fluoride ions and the reduction of acid production outside the cells (Koo, 2008; Marquis, 1995; ten Cate & van Loveren, 1999).

Although fluoride plays a significant role in the effective prevention of tooth decay, in line with widely extensive studies (dos Santos, Nadanovsky, & de Oliveira, 2013), the use of fluoride as a remineralization agent remains limited by its incomplete remineralization process, which is because fluoride causes the changes in the crystal structure, especially the surface layer of lesions (Silverstone, 1983), resulting in the blockage of fluoride permeability for subsurface remineralization with more difficulty (Kawasaki, 1989; Lammers, Borggreven, & Driessens, 1990; ten Cate & Featherstone, 1991). Besides, fluoride intake above the optimal fluoride level from birth until the first 6 years can result in dental fluorosis to the permanent teeth (Lalumandier & Rozier, 1995). It also causes acute toxicity from excessive fluoride intake with probably toxic doses in children or a certainly lethal dose in adults (Whitford, 1990).

Over the years, there have been more studies on hydroxyapatite nanoparticles, with biomimetic properties similar to hydroxyapatite crystals, the smallest subunit of the enamel layer in size, as well as chemical and crystal structures (Hannig & Hannig, 2010, 2012; Norberto Roveri et al., 2009). Calcium and phosphate of hydroxyapatite are important sources in the biomineralization process of hard tissues such as bones and teeth (Nudelman & Sommerdijk, 2012) by solubility and biocompatibility properties (Balasundaram, Sato, & Webster, 2006; Hu et al., 2007), with no toxicity and tissue inflammation. There are also nano-sized crystals, which help to increase the surface area of actions and adherences with a



concentration equal to micro-sized hydroxyapatite (Ginebra, Driessens, & Planell, 2004; Roveri & Iafisco, 2010). Therefore, an application concept of synthetic hydroxyapatite is suggested for the prevention and treatment of early dental caries, using calcium and phosphate ions from synthesized crystals for the remineralization of crystals being damaged by the demineralization process in the enamel.

Previous studies yielded the effectiveness of nanometer-grade synthetic hydroxyapatite crystals in the reparation and remineralization better than the micro-sized hydroxyapatite (Huang, Gao, Cheng, & Yu, 2011; Li et al., 2008). Currently, several studies are focused on the combination of nano-hydroxyapatite in oral care products to prevent dental cavities, such as toothpaste (Esteves-Oliveira, Santos, Meyer-Lueckel, Wierichs, & Rodrigues, 2017; Tschoppe et al., 2011), mouthwash (Kim, Kwon, Choi, & Kim, 2007), and paste (Comar, Souza, Gracindo, Buzalaf, & Magalhaes, 2013; Souza et al., 2015).

The nano-hydroxyapatite has two mechanisms of action in remineralization. First, it is a free source of calcium and phosphate ions based on intrinsic characteristics, such as size, chemical composition, and similar structures to enamel crystals, which are significantly important in the remineralization process, unlike the solely free ion solutions (Huang et al., 2011). Huang et al. studied the effect of hydroxyapatite concentrations on the efficacy of remineralization. It was found that the increasing concentrations resulted in a higher rate and amount of nano-hydroxyapatite precipitation from calcium and phosphate ion depositions for the remineralization process. The nano-hydroxyapatite concentration of 10% could be the optimum amount for the remineralization of the early caries lesion in the enamel (Huang, Gao, & Yu, 2009).

The second mechanism in the remineralization process of nano-hydroxyapatite is the ability to fill microscopic surface fissures in the surface of the demineralized enamel layer, causing the reduction of pores and defects (Huang et al., 2009). It can then inhibit the demineralization process by concealing the interprismatic space, which is an acid infiltrating channel to dissolve minerals in the subsurface (Li et al., 2008). Additionally, the nano-hydroxyapatite surface layer is able to absorb calcium and phosphate ions from the remineralizing solutions into the enamel for precipitating reactions and promoting growth and nucleation of crystals (Li et al., 2008; Onuma, Yamagishi, & Oyane, 2005). The adhesion of nano-hydroxyapatite to the enamel surface is due to its biocompatibility properties and approximate size to crystals in the enamel layer. Li et al. showed that the synthetic nanohydroxyapatite of 20 nm possesses similar properties to the building block of natural enamel crystals, resulting in higher affinity between them. Consequently, the adhesion remains superior even going through ultrasonic cleansing with ultrasonic treatment (Li et al., 2008). However, the new apatite layer with high mineral deposits may prevent the diffusion of free mineral ions into subsurface lesions, leading to the incomplete remineralization process with nano-hydroxyapatite (Huang et al., 2011).

Hence, the researchers are interested in using experimental nano-hydroxyapatite contained pastes due to their longer contact time with the teeth than toothpaste and mouthwash. In particular, it can be applied as home use rather than professional use. At present, few studies have compared the remineralization effects of nano-hydroxyapatite-containing pastes with different methods and measurements. The purpose of this study is to investigate the remineralization effects of experimental nano-hydroxyapatite-containing pastes on the early demineralized enamel under a simulated pH cycling model compared with fluoride-containing pastes, using direct mineral quantification.

## 2. Objectives

To evaluate the remineralization effects of a nano-hydroxyapatite paste on early demineralized enamel under simulated pH cycling model compare with a fluoride paste.

## 3. Materials and Methods

### 3.1 Preparation of enamel specimens

This study used human premolar teeth that were extracted for orthodontic treatment or tooth mobility from periodontitis. The study was approved for human research by the Faculty of Dentistry Human Experimentation Committee, Chiang Mai University, Thailand (Document No. 20/2562).

Human premolars were extracted for orthodontic treatment or tooth mobility from periodontitis with intact crown, no crack line, or caries lesion were obtained for the removal of tissue debris and calculus at the crown and root surface by ultrasonic, then stored in 0.1% thymol solution (Caelo, Hilden, Germany). Eighty



enamel specimens of a cubic shape of 4 x 4 x 3 (width x length x thickness) cubic millimeters were obtained from the buccal and lingual aspect of the tooth's crown, then the enamel specimens were embedded in acrylic resin blocks by custom-made mold. The enamel surface was polished using a grinding/polishing machine (MEGA Advance Co., Ltd., Shandong, China) at 600, 1000, 1500, and 2000 grits, respectively, with water for 1 minute at a speed of 100 rpm per each resolution to make the enamel into a flat surface with acrylic resin block surface. All of the polished specimens were cleaned with an ultrasonic cleanser (BioSonic UC125; Whaledent Inc, OH, USA) for 10 minutes.

### 3.2 Artificial demineralized enamel formation

The enamel specimen surface area was divided into three equal parts, with about 1.3 mm each in width, as the sound enamel control, the demineralized enamel control, and the treated enamel under pH cycling as shown in Figure 1.

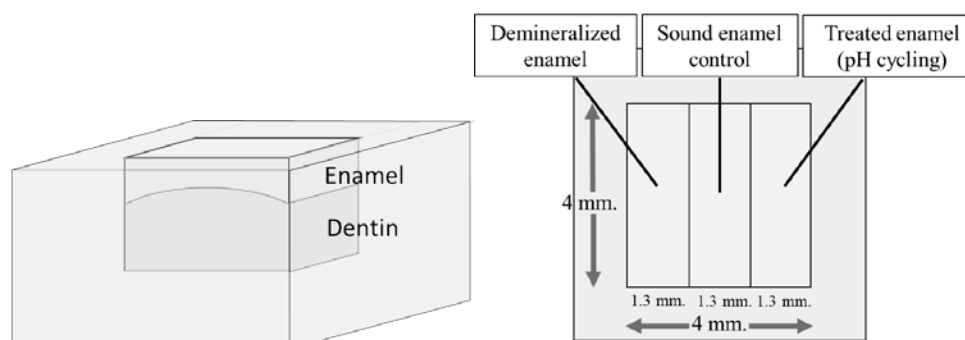


**Figure 1** Enamel specimens were embedded in acrylic resin blocks with a flat surface. When viewing from above, the enamel specimen area was divided into three parts as the sound enamel control, the demineralized enamel control, and the treated enamel under pH cycling

The center part was coated with nail varnish for the sound enamel control, then immersed in acetic acid buffer solution for the artificial demineralized enamel formation. The formula contained acetic acid 50 mmol (mM), calcium chloride ( $\text{CaCl}_2 \cdot 2\text{H}_2\text{O}$ ) 2.2 mM, potassium dihydrogen phosphate ( $\text{KH}_2\text{PO}_4$ ) 2.2 mM, and potassium fluoride 0.1 ppm, with pH 4.5 of 2 ml per specimens at 37°C for 7 days. A new solution was changed daily.

### 3.3 Measurement of demineralized enamel

After the artificial demineralized enamel formation, all specimens were cross-sectioned with a low-speed precision cutting machine (IsoMet™; BUEHLER, Illinois, USA) with a thickness of 1 mm for the first measurement, using micro-CT cross-section radiography imaging to analyze mineral density. The variables were mineral density profile (MD) to calculate lesion depth (LD) and mineral loss ( $\Delta Z$ ).

### 3.4 Measurement with micro-CT imaging

The cross-sectioned specimen was then analyzed for mineral density, using micro-CT cross-section radiography imaging (microCT35; SCANCO Medical AG, Brüttisellen, Switzerland) with the enamel surface perpendicular to the X-ray beam. The X-ray beam was 70 kV at 114  $\mu\text{A}$ . There were 4 pure hydroxyapatite slabs with a mineral density of 101, 211, 417, 790 milligram-hydroxyapatite per cubic centimeter (mgHAP/ccm) was scanned for setting to calibrate mineral density.

After scanning the cross-sectioned specimen, a stack of 8-bit grayscale images in the TIFF format at 1,024 x 1,024 pixels and 5.0  $\mu\text{m}$  voxel was quantitatively analyzed utilizing the imaging program (ImageJ; NIH, Bethesda, MD, USA). The grayscale value was changed to mineral density. The linear calibration curve obtained from the grayscale of pure hydroxyapatite was used for analysis. The calculated mean mineral



density values were defined for each depth as mineral density. The starting point of the depth axis was based on the enamel surface with the volume of interest at 100 x 200 x 1,200 cubic micrometers (thickness x width x depth), as part of the area to be measured.

The quantitatively analyzed data provided a set of data as the mineral density of normal enamel control ( $MD_B$ ) and the artificial demineralized enamel formation ( $MD_D$ ). Both data of mineral density were calculated resulting in lesion depth ( $LD_D$ ) and mineral loss ( $\Delta Z_D$ ) after the artificial demineralized enamel formation. The amount of mineral loss was calculated from the area under the graph between the mineral density of normal enamel and the mineral density of artificial demineralized enamel formation. The lesion depth was determined from the depth range of mineral volume at 95% of the maximum mineral density (Arends, Dijkman, & Christoffersen, 1987) as shown in Figure 2.

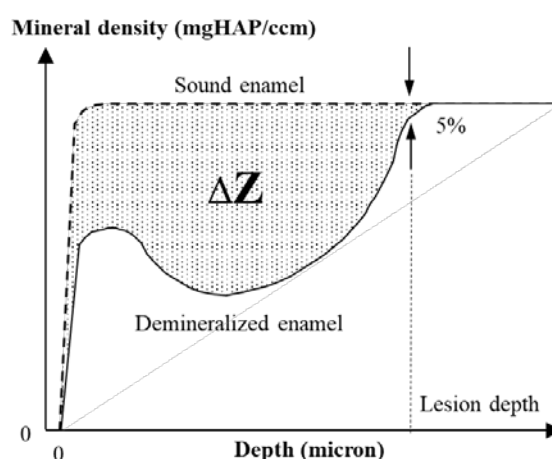


**Figure 2** The mineral loss ( $\Delta Z$ ) The mineral loss was calculated from the area between the dashed curve for the mineral density profile of sound enamel and the solid curve for the mineral density profile of demineralized enamel. The lesion depth was determined from the depth range of mineral volume at 95% of the maximum mineral density

### 3.5 Experimental and control groups

Forty-eight specimens were selected from the mineral density data. The specimens for inclusion needed to apparently have an intact surface layer, with a similar average volume of mineral loss ( $\Delta Z_D$ ) from the statistical calculation by cutting off 10 percent over the upper and lower border of the group (Lippert et al., 2011). The remaining part of selected specimens coated with nail varnish on the sectioned site. Another part of the enamel surface was coated with nail varnish to be preserved as the control of artificially demineralized enamel as shown in Figure 1. Then, the specimens were randomly selected and divided into 3 groups, with 16 specimens in each group, to test each remineralized agent-containing paste. Group 1 was the control group without treatment. Group 2 was the nH group with experimental nano-hydroxyapatite paste, containing 10% nano-hydroxyapatite (nanoX-im; Fluidinova, S.A., Moreira da Maia, Portugal). Group 3 was the F group with fluoride-containing paste, containing 1,000 ppm of sodium fluoride.

All groups utilized the same method for the pastes, using a brush (Microbrush®; Microbrush® International, WI, United States). The paste was applied on the wet enamel specimen for 5 minutes to simulate the application onto the enamel surface in the oral cavity without spoiling or swallowing. After that, the specimens were put in remineralized solutions for another 25 minutes to simulate the paste retention on the teeth without eating or drinking during this period. Finally, the specimens were washed thoroughly before entering the simulated pH cycling.



### 3.6 Simulated pH cycling

To evaluate the remineralization of all experimental groups, pH cycling was performed to simulate the cycle of demineralization and remineralization of the enamel in the oral cavity. The periods for remineralization solutions in each specimen were in accordance with the formula containing 130 mM of potassium chloride (KCl), 1.5 mM of calcium chloride ( $\text{CaCl}_2 \cdot 2\text{H}_2\text{O}$ ), 0.9 mM of potassium dihydrogen phosphate ( $\text{KH}_2\text{PO}_4$ ), and 20 mM of HEPES buffer. The pH 7.0 was applied for a total of 19 hours, including acid buffer solution for demineralization period according to the above formula of 4 hours and 2 intervals of 30 minutes each for applying the pastes as mentioned above. The first interval was done before the start of the demineralization period. The other interval was 12 hours apart from the first period. The solutions were replaced daily and repeated for measurement at 7 and 14 days.

### 3.7 Measurement of remineralization

The specimens were cross-sectioned to obtain a 1 mm thick enamel specimen. The treated enamel under pH cycling was evaluated by micro-CT cross-section radiograph imaging. The data of mineral density data of those specimens were obtained at 7 days ( $\text{MD}_7$ ) and 14 days ( $\text{MD}_{14}$ ) for the 2<sup>nd</sup> and 3<sup>rd</sup> measurements, respectively. The same setting was managed as the first measurement. The mineral density data of these specimens were compared with the sound enamel control to calculate the mineral loss and lesion depth at 7 days ( $\Delta Z_7$ ,  $\text{LD}_7$ ) and 14 days ( $\Delta Z_{14}$ ,  $\text{LD}_{14}$ ).

### 3.8 Data analysis and statistics

The measurement of remineralization effect on the treated enamel under pH cycling was based on the variable values compared with the demineralized enamel control. The changes in mineral loss ( $\Delta\Delta Z$ ) and lesion depth ( $\Delta\text{LD}$ ) were obtained at 7 and 14 days as shown in Table 1, the variables for measurement in each step of this experiment.

**Table 1** The variables and calculation formula for measurement in each step of the experiment

Variables	After demineralized enamel	After treatment 7 days	Changes in 7 days	After treatment 14 days	Changes in 14 days
Mineral loss	$\Delta Z_D^*$	$\Delta Z_7^*$	$\Delta\Delta Z_7$ ( $=\Delta Z_7 - \Delta Z_D$ )	$\Delta Z_{14}^*$	$\Delta\Delta Z_{14}$ ( $=\Delta Z_{14} - \Delta Z_D$ )
Lesion depth	$\text{LD}_D^*$	$\text{LD}_7^*$	$\Delta\text{LD}_7$ ( $=\text{LD}_7 - \text{LD}_D$ )	$\text{LD}_{14}^*$	$\Delta\text{LD}_{14}$ ( $=\text{LD}_{14} - \text{LD}_D$ )

\*Mineral loss ( $\Delta Z$ ) and lesion depth ( $\text{LD}$ ) calculated by enamel mineral density ( $\text{MD}$ ) at those periods compared with mineral density profile of normal enamel ( $\text{MD}_B$ )

All experimental data were collected for statistical analysis using SPSS statistics software version 20 (IBM Corporation, Armonk, NY, USA). The Shapiro-Wilk test was used for normal distribution tests in each group before analyzing the results. Within on experimental group, mineral loss ( $\Delta Z$ ) and lesion depth ( $\text{LD}$ ) after artificial demineralized enamel formation, and treatment 7 and 14 days were analyzed using one-way ANOVA with the Scheffe method. Changes in mineral loss ( $\Delta\Delta Z$ ) and lesion depth ( $\Delta\text{LD}$ ) after treatment for 7 and 14 days between the experimental group were analyzed using two-way ANOVA. All tests were performed at a 5% level of significance, with testing power at 80%.

## 4. Results and discussion

Eighty specimens were prepared for mineral loss measurement by micro-CT analysis and observed the enamel surface in all specimens after artificial demineralized enamel formation. To select specimens with comparable and homogeneous demineralization, artificial carious lesions with intact surfaces were selected, and 48 specimens with a mean ( $\pm\text{SD}$ ) baseline mineral loss ( $\Delta Z$ ) of  $139,687.22 \pm 26,593.20$  mgHAP/ $\text{m}^2$  and a mean lesion depth ( $\text{LD}$ ) of  $245.60 \pm 24.06$   $\mu\text{m}$  were chosen from the 80 specimens originally prepared.



Figure 3 shows an example of micro-CT imaging after the artificial demineralized enamel formation. The enamel formed a radiolucency layer of similar depth. The surface layer remained at the same level as that of the sound enamel. After using the paste with simulated pH cycling in each experimental group, the nano-hydroxyapatite paste and the fluoride paste increased the radiopaque in the subsurface layer over the period of use. The difference was that the fluoride paste had more radiopaque, starting from the innermost layer to the outermost layer, which resulted in the decreased depth of the radiolucency layer when compared with that after the artificial demineralized formation. The nano-hydroxyapatite paste had a depth of radiolucency layer similar to that before using the paste, with more radiopaque throughout the depth. The control group demonstrated more radiolucency with increased depth of the layer over the period of use and a lower level of the surface layer rather than sound enamel.

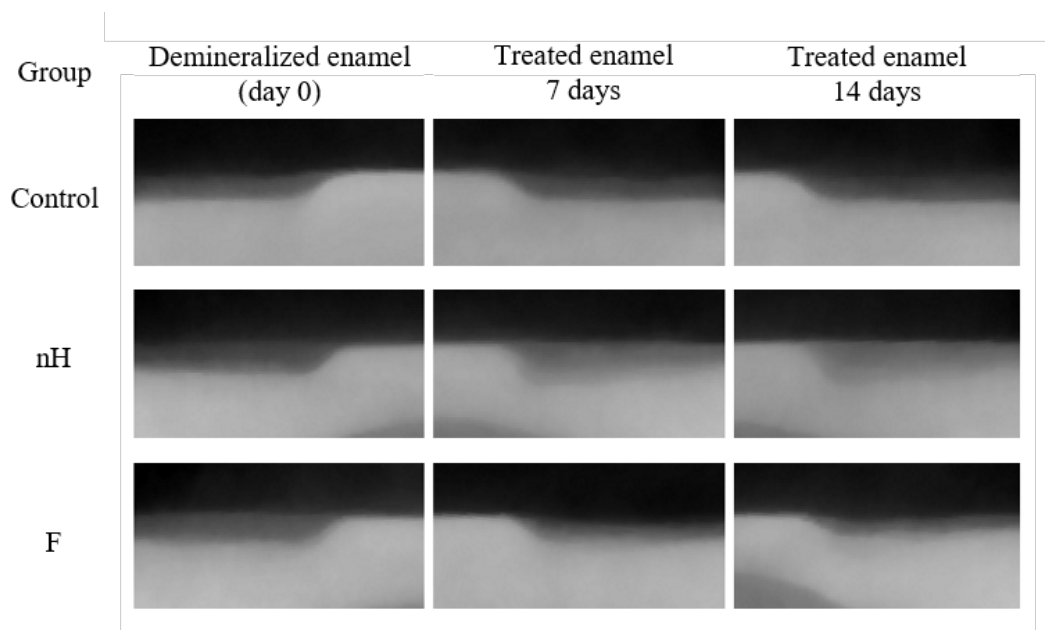


**Figure 3** An example of micro-CT images after demineralized enamel and treated enamel under pH cycling at 7 and 14 days in each experimental group

#### Measurement of mineral loss

For the mean mineral loss after the artificial demineralization for 7 and 14 days within each group, the control group showed a statistically significant increase in the mineral loss at 7 and 14 days compared to that after the artificial demineralized formation. Whilst, the nano-hydroxyapatite paste, and the fluoride paste yielded a statistically significant decrease in the mineral loss at 7 and 14 days (or the reversal of demineralization) compared to that after the artificial demineralized formation as shown in Table 2.

Regarding the comparison of mean change in the mineral loss at 7 and 14 days between the experimental group and the period of using the paste, it was found that the control group had a statistically significant increase of change in the mineral loss at the 14 days of simulated pH cycling. The nano-hydroxyapatite paste and the fluoride paste with the remineralization process had different values of change in mineral loss between the groups and the period of use. At 7 days, the nano-hydroxyapatite paste yielded a statistically significant less decrease change in mineral loss than the fluoride paste, then a similar decrease at 14 days with no statistically significant difference as shown in Table 3.



**Table 2** The mean and standard deviation of mineral loss (mgHAP/m<sup>2</sup>) in the experimental group with simulated pH cycling at different periods

Treatment group	$\Delta Z$ (mgHAP/ccm)		
	Demineralized enamel ( $\Delta Z_D$ )	day 7 ( $\Delta Z_7$ )	day 14 ( $\Delta Z_{14}$ )
control	123,260.28 $\pm$ 25,492.55 <sup>1</sup>	151,097.90 $\pm$ 24,628.33 <sup>2</sup>	173,402.85 $\pm$ 27,880.50 <sup>2</sup>
nH	147,453.86 $\pm$ 23,623.54 <sup>1</sup>	113,785.95 $\pm$ 22,472.05 <sup>2</sup>	95,057.58 $\pm$ 23,651.39 <sup>2</sup>
F	148,347.52 $\pm$ 23,995.18 <sup>1</sup>	123,118.17 $\pm$ 23,563.87 <sup>2</sup>	102,925.97 $\pm$ 26,161.19 <sup>2</sup>

Different numbers mean statistically significant differences in the mineral loss in the same group (row) at different periods ( $p < 0.05$ )

**Table 3** The mean and standard deviation of change in mineral loss (mgHAP/m<sup>2</sup>) in the experimental group with simulated pH cycling at different periods

Treatment group	$\Delta \Delta Z$ (mgHAP/ccm)		
	$\Delta \text{day 7}$ ( $\Delta \Delta Z_7$ )		$\Delta \text{day 14}$ ( $\Delta \Delta Z_{14}$ )
control	27,837.63 $\pm$ 5,469.05	D	50,142.57 $\pm$ 8,247.25
nH	-33,667.91 $\pm$ 3,436.31	B	-52,396.28 $\pm$ 6,710.49
F	-25,229.35 $\pm$ 5,037.03	C	-45,421.55 $\pm$ 6,609.59

Different capital letters mean statistically significant differences in the change in the mineral loss in different groups and periods ( $p < 0.05$ )

#### Lesion depth

When considering the experimental group with increased lesion depth over the period of using the paste, it was found that the control group had a statistically significant increase in lesion depth at 7 and 14 days compared to that after the artificial demineralized formation. The nano-hydroxyapatite paste and the fluoride paste were experimental groups with reduced lesion depth over the period of use. When comparing the mean lesion depth within the groups, the nano-hydroxyapatite paste exhibited a decrease in lesion depth. At 14 days, the lesion depth was lower compared with that after the period of demineralization and the 7 days of using this paste, with statistical significance. The fluoride paste had a continuously decreased lesion depth over time, with a statistically significant difference at the 3 periods as shown in Table 4.

**Table 4** The mean and standard deviation of lesion depth (micron) of the experimental group with simulated pH cycling simulations at different periods

Treatment group	LD (micron)		
	Demineralized enamel ( $LD_D$ )	day 7 ( $LD_7$ )	day 14 ( $LD_{14}$ )
control	242.22 $\pm$ 24.25 <sup>1</sup>	274.39 $\pm$ 22.98 <sup>2</sup>	286.08 $\pm$ 27.19 <sup>2</sup>
nH	246.59 $\pm$ 22.41 <sup>1</sup>	232.53 $\pm$ 22.13 <sup>1</sup>	204.49 $\pm$ 22.35 <sup>2</sup>
F	247.98 $\pm$ 26.55 <sup>1</sup>	223.01 $\pm$ 25.54 <sup>2</sup>	197.66 $\pm$ 29.32 <sup>3</sup>

Different numbers mean statistically significant differences in lesion depth in the same group (row) at different periods ( $p < 0.05$ ).

**Table 5** The mean and standard deviation of change in lesion depth (micron) of the experimental group with simulated pH cycling simulations at different periods

Treatment group	$\Delta LD$ (micron)		
	$\Delta \text{day 7}$ ( $\Delta LD_7$ )		$\Delta \text{day 14}$ ( $\Delta LD_{14}$ )
control	32.17 $\pm$ 6.50	E	43.87 $\pm$ 5.21
nH	-14.06 $\pm$ 2.18	D	-42.09 $\pm$ 5.60
F	-24.98 $\pm$ 3.38	C	-50.32 $\pm$ 7.11

Different capital letters mean statistically significant differences in the change of lesion depth in different groups and periods ( $p < 0.05$ ).



When comparing the mean change in lesion depth at 7 and 14 days between the experimental group and the period of use, it was found that the control group had a statistically significant increase change in lesion depth over time, unlike the nano-hydroxyapatite paste and the fluoride paste which showed a statistically significant decrease change in lesion depth over the period of use. At different periods of use, the fluoride paste demonstrated a statistically significant more decrease in lesion depth than that of the nano-hydroxyapatite paste as shown in Table 5.

In this study, micro-CT cross-section radiography imaging was used to measure the effectiveness of the paste to the early demineralized enamel with simulated pH cycling for the analysis of mineral loss and lesion depth of the demineralized enamel. Although the transverse microradiography technique is the gold standard method for determining mineral density volume (Ten Bosch & Angmar-Månsson, 1991), the micro-CT cross-section radiography imaging with higher resolution as a three-dimensional radiography technique of non-destructive intervention can nowadays be applied to analyze mineral density (Hamba, Nikaido, Sadr, Nakashima, & Tagami, 2012; Neves Ade, Coutinho, Vivan Cardoso, Jaecques, & Van Meerbeek, 2010). Also, it can be used to analyze mineral loss and lesion depth similar to the transverse microradiography technique (Arends et al., 1987). Thus, micro-CT cross-section radiography imaging becomes another method to evaluate the mineral density of the teeth.

The results of artificial demineralized enamel formation yielded all samples in this research as white spot lesions with intact outer surface and demineralized and porous subsurface, which are the characteristics of early demineralized enamel. The main factor causing these lesions in laboratory testing was acetic acid buffer solution which contained 0.1 ppm fluoride in the mechanism to inhibit demineralization. Fluoride binds to hydroxyapatite crystals at the enamel surface due to greater saturation of ion solution compared with fluorapatite crystals despite little concentration of fluoride ions (ten Cate & Duijsters, 1983a, 1983b). It formed an acid-resistant enamel layer that could dissolve minerals only in the subsurface and caused subsurface lesions.

The simulated pH cycling in this study resulted in the artificial demineralized enamel formation of the control group demonstrated that the effects of measurement by micro-CT yielded an increase in mineral loss and lesion depth over time. The simulated pH cycling in this experiment caused the total mineral loss similar to a study by ten Cate et al. at the demineralization and remineralization periods of 3 and 21 hours, respectively, in the artificial demineralized enamel formation with continuous mineral loss (ten Cate & Duijsters, 1982). It resulted from the demineralization period that used pH 4.5-free acid buffer solution to create the simulated acidic conditions from bacterial sugar digestion, causing the less saturated condition and dissolves fluorapatite at the surface layer of lesions after the artificial demineralized enamel formation (ten Cate & Featherstone, 1991). The surface layer was partially dissolved and was responsible for the prevention of dissolved mineral diffusion in the subsurface. The acid buffer solution could therefore promote more demineralization in the lesion layer.

Several studies reported that nano-hydroxyapatite possesses remineralization properties to the early demineralized enamel (Huang et al., 2011; Huang et al., 2009; Tschoppe et al., 2011). Nonetheless, there are few studies on the effects of nano-hydroxyapatite-containing pastes on the remineralization of demineralized enamel. Most of them demonstrated that the nano-hydroxyapatite-containing pastes could remineralize the primary demineralized enamel (Daas, Badr, & Osman, 2018; de Carvalho et al., 2014; Souza et al., 2015; Vyavhare, Sharma, & Kulkarni, 2015). The results of micro-CT in this study illustrated that the total remineralization could progress over the periods of using the paste under pH cycling due to the intrinsic properties of a nano-hydroxyapatite particle that could penetrate the pores in the demineralized enamel (Huang et al., 2009). It was also a source of calcium and phosphate-free ions, as an integral part of enamel remineralization (Huang et al., 2011). As a result, the micro-CT could demonstrate greater radiopacity throughout the lesion depth, indicating the early remineralization close to the outermost layer before entering the inner lesion layer and according to a study by Huang et al (S. Huang, Gao, Cheng, & Yu, 2010), due to the small size of nano-hydroxyapatite that penetrated and filled the defects and pores close to the outer layer rather than the inner layer of lesions, following the size and pore volume in each area of enamel caries (Featherstone, 2008).



The period of mineral loss in simulated pH cycling simulation also influenced the amount of calcium and phosphate ions released from nano-hydroxyapatite. Since the solubility of nano-hydroxyapatite was increased in the acidic conditions, it was consistent with a study that showed a significantly greater release of calcium and phosphate ions from nano-hydroxyapatite at pH 4 compared to pH 7. The increasing of free ions had positive effects on the remineralization of dental caries in both lesion depth and mineral volume (Huang et al., 2011), which ultimately may cause greater remineralization rather than demineralization.

The fluoride contained paste would be able to promote the total remineralization when using in accordance with simulated pH cycling over time, which is because fluoride maintains the ability to inhibit demineralization by combining with hydroxyapatite to become fluorapatite of higher resistance to dissolution than hydroxyapatite. It also promotes remineralization by attracting calcium and phosphate ions to create crystals for replacement of the loss (Buzalaf et al., 2011; Robinson, 2009). The micro-CT images illustrated that the remineralization starts from the innermost layer of lesions to the outer layer, which is different from that of the experimental nano-hydroxyapatite containing pastes to cause early changes at the outer layer before penetrating the inner lesion. In a study on the chemistry of enamel caries by Robinson et al., it was found that during the period of early demineralization, the translucent zone and dark zone are areas of high carbonate and magnesium concentrations since both are unstable with easy dissolution (Robinson et al., 2000). Fluoride has the ability to penetrate the lesion layer through space and repair the crystals for carbonate and magnesium replacement (Robinson, 2009). It produces a more stable crystal appearance, with higher resistance to acids and greater hardness than hydroxyapatite (Pajor, Pajchel, & Kolmas, 2019). Hence, there is a decrease in lesion depth in the experimental fluoride-containing paste over the period of use, with more statistical significance than the nano-hydroxyapatite paste.

## 5. Conclusion

Following the scope of this study, the use of nano-hydroxyapatite paste under the condition of pH-cycling for 14 days promotes remineralization on early demineralized enamel in the same way as using fluoride paste. However, the different characteristics of remineralization should be observed.

## 6. Acknowledgements

The authors are grateful to the Faculty of Dentistry, Prince of Songkla University for their help with the micro-CT scan.

## 7. References

- Adair, S. M. (2006). Evidence-based use of fluoride in contemporary pediatric dental practice. *Pediatr Dent*, 28(2), 133-142; discussion 192-138.
- Arends, J., & Christoffersen, J. (1990). Nature and role of loosely bound fluoride in dental caries. *J Dent Res*, 69(suppl 2), 601-605; discussion 634-606. doi:10.1177/00220345900690s118
- Arends, J., Dijkman, T., & Christoffersen, J. (1987). Average mineral loss in dental enamel during demineralization. *Caries Res*, 21(3), 249-254. doi:10.1159/000261028
- Balasundaram, G., Sato, M., & Webster, T. J. (2006). Using hydroxyapatite nanoparticles and decreased crystallinity to promote osteoblast adhesion similar to functionalizing with RGD. *Biomaterials*, 27(14), 2798-2805. doi:10.1016/j.biomaterials.2005.12.008
- Bruun, C., Bille, J., Hansen, K. T., Kann, J., Qvist, V., & Thylstrup, A. (1985). Three-year caries increments after fluoride rinses or topical applications with a fluoride varnish. *Community Dent Oral Epidemiol*, 13(6), 299-303.
- Bruun, C., Lambrou, D., Larsen, M. J., Fejerskov, O., & Thylstrup, A. (1982). Fluoride in mixed human saliva after different topical fluoride treatments and possible relation to caries inhibition. *Community Dent Oral Epidemiol*, 10(3), 124-129.
- Buzalaf, M. A., Pessan, J. P., Honorio, H. M., & ten Cate, J. M. (2011). Mechanisms of action of fluoride for caries control. *Monogr Oral Sci*, 22, 97-114. doi:10.1159/000325151



- Cochrane, N. J., Cai, F., Huq, N. L., Burrow, M. F., & Reynolds, E. C. (2010). New approaches to enhanced remineralization of tooth enamel. *J Dent Res*, *89*(11), 1187-1197. doi:10.1177/0022034510376046
- Comar, L.P., Souza, B.M., Gracindo, L.F., Buzalaf, M.A., & Magalhaes, A.C. (2013). Impact of experimental nano-HAP pastes on bovine enamel and dentin submitted to a pH cycling model. *Braz Dent J*, *24*(3), 273-278. doi:10.1590/0103-6440201302175
- Daas, I., Badr, S., & Osman, E. (2018). Comparison between fluoride and nano-hydroxyapatite in remineralizing initial enamel lesion: an in vitro study. *J Contemp Dent Pract*, *19*(3), 306-312.
- de Carvalho, F. G., Vieira, B. R., Santos, R. L., Carlo, H. L., Lopes, P. Q., & de Lima, B. A. (2014). In vitro effects of nano-hydroxyapatite paste on initial enamel carious lesions. *Pediatr Dent*, *36*(3), 85-89.
- dos Santos, A. P., Nadanovsky, P., & de Oliveira, B. H. (2013). A systematic review and meta-analysis of the effects of fluoride toothpastes on the prevention of dental caries in the primary dentition of preschool children. *Community Dent Oral Epidemiol*, *41*(1), 1-12. doi:10.1111/j.1600-0528.2012.00708.x
- Esteves-Oliveira, M., Santos, N. M., Meyer-Lueckel, H., Wierichs, R. J., & Rodrigues, J. A. (2017). Caries-preventive effect of anti-erosive and nano-hydroxyapatite-containing toothpastes in vitro. *Clin Oral Investig*, *21*(1), 291-300. doi:10.1007/s00784-016-1789-0
- Featherstone, J. D. (1999). Prevention and reversal of dental caries: role of low level fluoride. *Community Dent Oral Epidemiol*, *27*(1), 31-40.
- Featherstone, J. D. (2000). The science and practice of caries prevention. *J Am Dent Assoc*, *131*(7), 887-899.
- Featherstone, J.D. (2008). Dental caries: a dynamic disease process. *Aust Dent J*, *53*(3), 286-291. doi:10.1111/j.1834-7819.2008.00064.x
- Featherstone, J. D., Glena, R., Shariati, M., & Shields, C. P. (1990). Dependence of in vitro demineralization of apatite and remineralization of dental enamel on fluoride concentration. *J Dent Res*, *69*(suppl 2), 620-625; discussion 634-626. doi:10.1177/00220345900690s121
- Ginebra, M.P., Driessens, F.C., & Planell, J.A. (2004). Effect of the particle size on the micro and nanostructural features of a calcium phosphate cement: a kinetic analysis. *Biomaterials*, *25*(17), 3453-3462. doi:10.1016/j.biomaterials.2003.10.049
- Hamba, H., Nikaido, T., Sadr, A., Nakashima, S., & Tagami, J. (2012). Enamel lesion parameter correlations between polychromatic micro-CT and TMR. *J Dent Res*, *91*(6), 586-591. doi:10.1177/0022034512444127
- Hannig, M., & Hannig, C. (2010). Nanomaterials in preventive dentistry. *Nat Nanotechnol*, *5*(8), 565-569. doi:10.1038/nnano.2010.83
- Hannig, M., & Hannig, C. (2012). Nanotechnology and its role in caries therapy. *Adv Dent Res*, *24*(2), 53-57. doi:10.1177/0022034512450446
- Hu, Q., Tan, Z., Liu, Y., Tao, J., Cai, Y., Zhang, M., Tang, R. (2007). Effect of crystallinity of calcium phosphate nanoparticles on adhesion, proliferation, and differentiation of bone marrow mesenchymal stem cells. *J Mater Chem*, *17*(44), 4690-4698. doi:10.1039/B710936A
- Huang, S., Gao, S., Cheng, L., & Yu, H. (2010). Combined effects of nano-hydroxyapatite and *Galla chinensis* on remineralisation of initial enamel lesion in vitro. *J Dent*, *38*(10), 811-819. doi:10.1016/j.jdent.2010.06.013
- Huang, S.B., Gao, S.G., S.S., Cheng, L., & Yu, H.Y. (2011). Remineralization potential of nano-hydroxyapatite on initial enamel lesions: an in vitro study. *Caries Res*, *45*(5), 460-468. doi:10.1159/000331207
- Huang, S.B., Gao, S.S., & Yu, H.Y. (2009). Effect of nano-hydroxyapatite concentration on remineralization of initial enamel lesion in vitro. *Biomed Mater*, *4*(3), 034104. doi:10.1088/1748-6041/4/3/034104
- Kawasaki, K. (1989). Effect of carboxymethylcellulose on fluoride uptake and remineralization in demineralized enamel. *J Dent Hlth*, *39*(2), 242-255. doi:10.5834/jdh.39.242



- Kidd, E. A., & Fejerskov, O. (2004). What constitutes dental caries? Histopathology of carious enamel and dentin related to the action of cariogenic biofilms. *J Dent Res*, 83(suppl 1), 35-38.
- Kim, M. Y., Kwon, H. K., Choi, C. H., & Kim, B. I. (2007). Combined effects of nano-hydroxyapatite and NaF on remineralization of early caries lesion. *Key Eng Mater*, 330-332 II, 1347-1350.
- Koo, H. (2008). Strategies to enhance the biological effects of fluoride on dental biofilms. *Adv Dent Res*, 20(1), 17-21. doi:10.1177/154407370802000105
- Lalumandier, J. A., & Rozier, R. G. (1995). The prevalence and risk factors of fluorosis among patients in a pediatric dental practice. *Pediatr Dent*, 17(1), 19-25.
- Lammers, P. C., Borggreven, J. M., & Driessens, F. C. (1990). Influence of fluoride on in vitro remineralization of artificial subsurface lesions determined with a sandwich technique. *Caries Res*, 24(2), 81-85. doi:10.1159/000261244
- Li, L., Pan, H., Tao, J., Xu, X., Mao, C., Gu, X., & Tang, R. (2008). Repair of enamel by using hydroxyapatite nanoparticles as the building blocks. *J Mater Chem*, 18(34), 4079-4084. doi:10.1039/B806090H
- Lippert, F., Lynch, R. J., Eckert, G. J., Kelly, S. A., Hara, A. T., & Zero, D. T. (2011). In situ fluoride response of caries lesions with different mineral distributions at baseline. *Caries Res*, 45(1), 47-55. doi:10.1159/000323846
- Marquis, R. E. (1995). Antimicrobial actions of fluoride for oral bacteria. *Can J Microbiol*, 41(11), 955-964.
- Moreno, E. C., & Zahradnik, R. T. (1973). The pore structure of human dental enamel. *Arch Oral Biol*, 18(8), 1063-1068.
- Murdoch-Kinch, C. A., & McLean, M. E. (2003). Minimally invasive dentistry. *J Am Dent Assoc*, 134(1), 87-95.
- Neves Ade, A., Coutinho, E., Vivian Cardoso, M., Jaecques, S. V., & Van Meerbeek, B. (2010). Micro-CT based quantitative evaluation of caries excavation. *Dent Mater*, 26(6), 579-588. doi:10.1016/j.dental.2010.01.012
- Nudelman, F., & Sommerdijk, N. A. (2012). Biomineralization as an inspiration for materials chemistry. *Angew Chem Int Ed Engl*, 51(27), 6582-6596. doi:10.1002/anie.201106715
- Odutuga, A. A., & Prout, R. E. (1974). Lipid analysis of human enamel and dentine. *Arch Oral Biol*, 19(8), 729-731.
- Onuma, K., Yamagishi, K., & Oyane, A. (2005). Nucleation and growth of hydroxyapatite nanocrystals for nondestructive repair of early caries lesions. *J Cryst Growth*, 282(1), 199-207. doi:10.1016/j.jcrysgro.2005.04.085
- Pajor, K., Pajchel, L., & Kolmas, J. (2019). Hydroxyapatite and fluorapatite in conservative dentistry and oral implantology-a review. *Materials (Basel)*, 12(17). doi:10.3390/ma12172683
- Pitts, N. B. (2004). Modern concepts of caries measurement. *J Dent Res*, 83(suppl 1), C43-47.
- Robinson, C. (2009). Fluoride and the caries lesion: interactions and mechanism of action. *Eur Arch Paediatr Dent*, 10(3), 136-140.
- Robinson, C., Shore, R. C., Brookes, S. J., Strafford, S., Wood, S. R., & Kirkham, J. (2000). The chemistry of enamel caries. *Crit Rev Oral Biol Med*, 11(4), 481-495.
- Roveri, N., Battistella, E., Bianchi, C., Foltran, I., Foresti, E., Iafisco, M., . . . Rimondini, L. (2009). Surface enamel remineralization: biomimetic apatite nanocrystals and fluoride ions different effects. *J Nanomater*, 2009, 8. doi:10.1155/2009/746383
- Roveri, N., & Iafisco, M. (2010). Evolving application of biomimetic nanostructured hydroxyapatite. *Nanotechnol Sci Appl*, 3, 107-125. doi:10.2147/nsa.S9038
- Silverstone, L.M. (1983). Remineralization and enamel caries: new concepts. *Dent Update*, 10(4), 261-273.
- Souza, B. M., Comar, L. P., Vertuan, M., Fernandes Neto, C., Buzalaf, M. A., & Magalhaes, A. C. (2015). Effect of an experimental paste with hydroxyapatite nanoparticles and fluoride on dental demineralisation and remineralisation in situ. *Caries Res*, 49(5), 499-507. doi:10.1159/000438466
- Ten Bosch, J.J., & Angmar-Månsson, B. (1991). A review of quantitative methods for studies of mineral content of intra-oral caries lesions. *J Dent Res*, 70(1), 2-14. doi:10.1177/00220345910700010301



- ten Cate, J.M., & Duijsters, P.P. (1982). Alternating demineralization and remineralization of artificial enamel lesions. *Caries Res*, *16*(3), 201-210. doi:10.1159/000260599
- ten Cate, J.M., & Duijsters, P.P. (1983a). Influence of fluoride in solution on tooth demineralization. I. Chemical data. *Caries Res*, *17*(3), 193-199. doi:10.1159/000260667
- ten Cate, J.M., & Duijsters, P.P. (1983b). Influence of fluoride in solution on tooth demineralization. II. Microradiographic data. *Caries Res*, *17*(6), 513-519. doi:10.1159/000260711
- ten Cate, J.M., & Featherstone, J.D. (1991). Mechanistic aspects of the interactions between fluoride and dental enamel. *Crit Rev Oral Biol Med*, *2*(3), 283-296.
- ten Cate, J.M., & van Loveren, C. (1999). Fluoride mechanisms. *Dent Clin North Am*, *43*(4), 713-742, vii.
- Tschoppe, P., Zandim, D. L., Martus, P., & Kielbassa, A. M. (2011). Enamel and dentine remineralization by nano-hydroxyapatite toothpastes. *J Dent*, *39*(6), 430-437. doi:10.1016/j.jdent.2011.03.008
- Vyavhare, S., Sharma, D. S., & Kulkarni, V. K. (2015). Effect of three different pastes on remineralization of initial enamel lesion: an in vitro study. *J Clin Pediatr Dent*, *39*(2), 149-160.
- Whitford, G.M. (1990). The physiological and toxicological characteristics of fluoride. *J Dent Res*, *69*(suppl 2), 539-549; discussion 556-537. doi:10.1177/00220345900690s108
- Yamagishi, K., Onuma, K., Suzuki, T., Okada, F., Tagami, J., Otsuki, M., & Senawangse, P. (2005). Materials chemistry: a synthetic enamel for rapid tooth repair. *Nature*, *433*(7028), 819. doi:10.1038/433819a